A NUMERICAL STUDY OF INCOMPRESSIBLE FLOW PROBLEMS OF NON-NEWTONIAN OR TURBULENT TYPE

M.F. WEBSTER

Numerical Analysis Report 13/85

This work forms part of the research programme of the Institute for Computational Fluid Dynamics at the Universities of Oxford and Reading.

Summary

A finite difference numerical technique is presented to solve equations of Navier-Stokes type when coupled with a stress equation. Steady planar two-dimensional flows of incompressible non-Newtonian and turbulent fluid models are considered. The system of nonlinear equations that results is solved iteratively using a successive substitution approach that introduces a set of linear equations and a combination of inner and outer iterations.

The convergence of the iteration and the stability of the difference scheme are analysed for a forward-facing step problem. Particular attention is paid to the dependence of the outer iteration upon the relevant material parameters. Results are presented for the second-order Non-Newtonian model and an extension is developed to enable the scheme to deal with a $k\sim\ell$ turbulence model.

1. Introduction

(i) Scope of Paper

A numerical scheme is presented which solves equations of Navier-Stokes type for steady planar two-dimensional incompressible flows. The flow variables considered are stream function ψ, vorticity ω and stress ζ. The equation system to be solved is then stated in non-dimensional form as

$$\nabla^2\psi = -\omega, \tag{1a}$$

$$\nabla^2\omega = R\underset{\sim}{u}.\nabla\omega + W\underset{\sim}{u}.\nabla\zeta, \tag{1b}$$

with the definition of velocity $\underset{\sim}{u} = \nabla \times \psi = \left(\frac{\partial\psi}{\partial y}, -\frac{\partial\psi}{\partial x}\right)$ and where R is a Reynolds number and W a stress parameter (W is a Weissenberg number for the Non-Newtonian fluid model). Equation system (1) is completed by a stress description equation. Attention has initially been directed towards a stress term that arises in a simple Non-Newtonian fluid model where

$$\zeta = \nabla^2\omega \ . \tag{2}$$

This description is derived from the so-called second-order model. It is an overall aim that the techniques proposed should be sufficiently general to find application in any flow situation that may be described by a coupled system of the incompressible flow equations and a stress equation system. The Maxwell/Oldroyd models [1], some models for turbulent flows and buoyancy driven flows are all obvious candidates.

The full system of equations (1) and (2) is considered in a form with (1b) replaced by

$$W\underset{\sim}{u}.\nabla\zeta - \zeta = -R\underset{\sim}{u}.\nabla\omega \ , \tag{3}$$

representing two elliptic Poisson equations and a hyperbolic equation.

It is discretised by finite difference methods on a uniform grid: the usual five-point operator is used for (1a) and (2) with (3) replaced by a Crank-Nicolson type scheme. The resulting system of (nonlinear) equations is

solved iteratively in a sequence of Picard-type iterations at the outer or nonlinear level. At the linear or inner level a combination of inner iterations for the elliptic equations (SOR) and direct marching scheme for the hyperbolic equation is used. The convergence of the iteration and the stablility of the difference schemes are analysed for a forward-facing step problem. Results are given for various model problems covering a range of values for the two-parameter family (R,W).

(ii) Historical Background

The full system of nonlinear equations is solved iteratively. This paper concentrates on a traditional approach of linearisation by decoupling, introducing a set of linear equations and an outer Picard-type iteration. The present iterative scheme is compared to two similar iterative schemes proposed by Crochet and Pilate (2) and Davies (3). With integer $n \geq 0$ indicating an outer iteration number these schemes may be summarised as follows:

$$W\underset{\sim}{u}^{n}.\underset{\sim}{\nabla}(\nabla^2\omega^{r_1}) + R\underset{\sim}{u}^{n}.\underset{\sim}{\nabla}\omega^{r_2} - \nabla^2\omega^{r_3} = 0 , \qquad (4a)$$

$$\nabla^2\psi^{n+1} + \omega^{n+1} = 0 , \ \underset{\sim}{u}^{n+1} = \underset{\sim}{\nabla} \times \psi^{n+1} , \qquad (4b)$$

where for Scheme 1 (Crochet) $r_1 = r_2 = r_3 = n+1$; Scheme 2 (Davies) $r_1 = n$, $r_3 = n+1$, $R \equiv 0$; Scheme 3 (Present) $r_1 = r_3 = n+1$, $r_2 = n$.

Scheme 1 yields a third-order differential equation for ω leading to convergence difficulties in the corresponding inner iteration. Converged solutions of the outer iteration were reported for the values (R,W) of {(1,.1), (10,.2), (100,.4), (500,.8), (1000,1.4)}. A critical upper limit on W was observed for each selected R value, though this limit increased with increase in R. Scheme 2, with $R = 0$, gives an efficient inner ω iteration but W is effectively limited by the numerical smoothing of the source term $W\underset{\sim}{u}^{n}.\underset{\sim}{\nabla}(\nabla^2\omega^{n})$. Converged solutions were reported for (R,W) of {(0,.1), without filtering; (0,W), $W \leq 10$ with filtering}. The third and present scheme differs from schemes 1 and 2 by the inclusion of a three-step outer iteration, and the solution for $\nabla^2\omega$ at the linear level by a direct marching scheme. No upper limit on W is found for converged solutions for $R \leq 10$, though scheme 3 is dependent upon restriction of R.

The dependence of the outer iteration on R and W may be investigated through a linearised perturbation analysis using a single Fourier mode (see Morton et al., [4]). It may be deduced that low frequencies (i.e. long wavelengths) $|\underset{\sim}{\kappa}|$ give convergence difficulties for all three schemes. Scheme 2 also suffers at high frequencies leading to a bound on $|\underset{\sim}{\kappa}| \propto W^{-1}$ (see Tanner [5]) and convergence difficulties with increasing W. For scheme 1 at fixed R, as W increases from zero a limiting value may be predicted $W \propto R\,|\underset{\sim}{\kappa}|^{-2}_{min}$ which will increase with R. The present scheme presents much less severe restrictions on W for small R, but the situation is expected to deteriorate more rapidly with increasing R.

Acceptability of converged solutions for small R is based upon the Tanner/Geisekus theorem, (see Tanner [6]), for creeping flow ($R = 0$). At $W = 0$ the solution for ζ is trivial, $\zeta = \nabla^2\omega = 0$, and from Tanner's theorem the velocity field $\{\underset{\sim}{u}\}_{W=0}$ also satisfies the problem $\forall\ W > 0$.

2. Full Statement of Model Problem

The solution of the forward-facing step or contraction geometry is considered for the model equations discussed earlier and used in the following form:

$$W\underset{\sim}{u}^n.\underset{\sim}{\nabla}\zeta^{n+1} - \zeta^{n+1} = - R\underset{\sim}{u}^n.\underset{\sim}{\nabla}\omega^n \ , \tag{5a}$$

$$\nabla^2\omega^{n+1} = \zeta^{n+1} \ , \tag{5b}$$

$$\nabla^2\psi^{n+1} = - \omega^{n+1} \ , \ \underset{\sim}{u}^{n+1} = \underset{\sim}{\nabla} \times \psi^{n+1} = (u,v)^{n+1} \ . \tag{5c}$$

The region of solution is shown in Fig. 1: ABCD is a fixed boundary, FE a symmetry boundary, AF the inlet boundary and DE the outlet. The flow is assumed to be fully-developed at inlet and outlet. With, firstly, a statement of the minimum boundary assumptions required, followed by the implied conditions actually used, the appropriate boundary conditions are

Fixed boundary ABCD

$$u = v = 0 \implies \psi = 0 \ , \ \omega = - \frac{\partial^2\psi}{\partial n^2} \ , \ \zeta = 0 \ ; \tag{6a}$$

Inflow boundary AF

$$u \text{ given} \ , \ v = \frac{\partial v}{\partial x} = 0 \implies \psi \ , \ \omega \text{ given} \ ; \tag{6b}$$

Outflow Boundary DE

$$v = 0 \ , \ \frac{\partial \omega}{\partial x} = \frac{\partial \zeta}{\partial x} = 0 \implies \frac{\partial \psi}{\partial x} = \frac{\partial \omega}{\partial x} = 0 \ , \ \zeta = 0 \ ; \tag{6c}$$

Symmetry boundary EF

$$\frac{\partial u}{\partial y} = 0 \ , \quad v = 0 \quad \Longrightarrow \quad \psi = \text{constant}, \ \omega = 0 \ , \ \zeta = 0 \ . \qquad (6d)$$

For given values of R and W, the last remaining parameter in the problem is the step ratio AF:DE taken as 4:1.

Commencing from $W = 0$ for (5) and introducing small $W > 0$ involves consideration of a singular perturbation problem. One may expect boundary layers for ζ to result dependent upon the boundary conditions imposed. If a zero value of ζ is imposed at outlet then boundary layers are avoided. This is consistent with the exponetially decreasing complementary function form for ζ when treated as an ODE along the streamlines in the upstream direction.

3. Numerical Approximation

(i) Finite Difference Equations

The region Ω of Fig. 1 is covered by a regular square grid of side h and nodal values of the variables ψ, ω, ζ are denoted by $\psi_{i,j}$ etc. at nodes $x = ih$, $y = jh$. Values of h of $\frac{1}{8}$ and $\frac{1}{16}$ are used, with some 1400 mesh points and 16 mesh lengths at inflow for the former choice. Use is made of standard difference operator notation as follows:

$$\delta_x \psi_{i+\frac{1}{2},j} = \psi_{i+1,j} - \psi_{i,j} \quad ; \quad \mu_x \psi_{i+\frac{1}{2},j} = \tfrac{1}{2}(\psi_{i+1,j} + \psi_{i,j}) \qquad (7)$$

with similar meaning for δ_y and μ_y. The difference approximations for the Poisson equations for ω and ψ (5 b,c) are then

$$(\delta_x^2 + \delta_y^2)\, \omega_{i,j}^{n+1} = h^2 \zeta_{i,j}^{n+1} \quad ; \quad (\delta_x^2 + \delta_y^2)\, \psi_{i,j}^{n+1} = - h^2 \omega_{i,j}^{n+1} \ , \qquad (8)$$

the standard five-point schemes: here superscript (n+1) denotes the stage of the outer iteration process, $\zeta^{n+1} \longrightarrow \omega^{n+1} \longrightarrow \psi^{n+1}$.

Two different schemes are used for the stress equation (5 a): the box scheme in the recirculating flow region Ω_h^1 and the Crank-Nicolson type scheme in Ω_h^2 where the flow is predominantly in the x-direction. For the former, velocities are required at the centre of each cell and are given by the four-point formulae

$$u^n_{i+\frac{1}{2},j+\frac{1}{2}} = \frac{\mu_x}{h} \delta_y \psi^n_{i+\frac{1}{2},j+\frac{1}{2}} \ , \quad v^n_{i+\frac{1}{2},j+\frac{1}{2}} = - \frac{\mu_y}{h} \delta_x \psi^n_{i+\frac{1}{2},j+\frac{1}{2}} \ . \qquad (9a)$$

The box scheme approximation to (5 a) is

$$W\left[(u^n\mu_y\delta_x + v^n\mu_x\delta_y)\,\zeta^{n+1}\right]_{i+\frac{1}{2},j+\frac{1}{2}} - h\left[\theta\mu_x\mu_y\zeta_{i+\frac{1}{2},j+\frac{1}{2}} + (1-\theta)\zeta_{i,j+1}\right]^{n+1} \qquad (9b)$$

$$= -R\left[(u^n\mu_y\delta_x + v^n\mu_x\delta_y)\omega^n\right]_{i+\frac{1}{2},j+\frac{1}{2}}$$

where the parameter θ permits weighting within the scheme on a pointwise basis and ensures stability for all possible velocity fields. The Crank-Nicolson scheme covers two neighbouring cells with the same x-coordinates and is therefore centred at $(i+\frac{1}{2},j)$: thus the velocities are given by the unsymmetric formulae

$$u^n_{i+\frac{1}{2},j} = \frac{\mu_x}{h}\,\mu_y\,\delta_y\,\psi^n_{i+\frac{1}{2},j} \quad , \quad v^n_{i+\frac{1}{2},j} = -\frac{\delta_x}{h}\,\psi^n_{i+\frac{1}{2},j} \quad ; \qquad (10a)$$

and the approximation to (5 a) is

$$\left[W(u^n\delta_x + v^n\mu_x\mu_y\delta_y)\zeta^{n+1} - h\hat{\zeta}^{n+1}\right]_{i+\frac{1}{2},j} = -R\left[u^n\delta_x + v^n\mu_x\mu_y\delta_y)\omega^n\right]_{i+\frac{1}{2},j} \qquad (10b)$$

where $\hat{\zeta}_{i+\frac{1}{2},j} = \beta\zeta_{i+1,j} + (1-\beta)\,\zeta_{i,j}$. (10c)

The weighting parameter β is introduced to again ensure stability of the scheme for all velocity fields.

(ii) Boundary Condition Implementation

For the stream function ψ^n in (8), Dirichlet boundary conditions apply over the whole boundary except DE , from (6a,b,d). From (6c) Neumann conditions apply on DE (same for ω^n) and are incorporated in the following fashion:

$$\psi^n_{I,j} = \psi^n_{I-1,j} \quad , \quad \omega^n_{I,j} = \omega^n_{I-1,j} \; . \qquad (11)$$

Likewise for ω^n in (8) Dirichlet conditions apply on AF and EF from (6 b,d); only the specification of ω^n on the wall ABCD remains. This approximation is achieved by Taylor series expansions based on local wall velocity conditions. With reference to Fig. 2, use is made of the following derived formulae:

$$\omega^n_{i,J} = -2h^{-2}(\psi_{i,J+1} - \psi_{i,J})^{n-1}, \qquad (12a)$$

$$\omega^n_{i,J} = -3h^{-2}(\psi_{i,J+1} - \psi_{i,J})^{n-1} + .5\,\omega^r_{i,J+1} \; , \qquad (12b)$$

$$\omega^n_{I,J} = -2h^{-2}(\psi_{I-1,J} + \psi_{I,J+1} - 2\,\psi_{I,J})^{n-1} \; , \qquad (12c)$$

where I and J are wall coordinates, (I,J) is the re-entrant corner point C, and r in (12 b) may be chosen at level n-1 or n. Formula

(12 a) is formally first-order accurate, see (Thom [7]); formula (12 b) is second-order accurate, see Woods [8], and is used with $r = n$ at all wall points bar C; formula (12 c) is attributed to Kawaguti [9] and provides a finite estimate of ω_C^n based on the first-order form. At C, ω is unbounded; however the simple formula (12 c) generates an estimate closely approximating that provided by an asymptotic expansion matching scheme (see Holstein and Paddon [10]).

For stability reasons the equations for ζ^{n+1} in (10 b) are integrated from outflow to inflow, and from (6 a,c,d) ζ^{n+1} is set to zero on all boundaries, except on the inflow boundary AF. Fully-developed conditions at inflow provide a compatability check on the solution generated and for consistency ζ^{n+1} should decay and vanish there. Providing the exit length CD is sufficiently large no boundary layers are encountered, and in fact with $R \equiv 0$, then $\zeta \equiv 0 \; \forall \; W \geq 0$ as it should be. If the Crank-Nicolson scheme (10) were to be used over the whole region Ω_h sufficient data would now be available with $\{\omega,\psi\}_{i,j}^n$ specified at all interior and boundary points: the same is also true if the box scheme (9) is incorporated in a limited zone Ω_h^1 based on ABC but not extending across to the symmetry boundary EF.

4. Solution Procedure

The nonlinear equation system is decoupled into a system of three linear equations. A three-step outer Picard-type iteration is introduced where each step constitutes the solution of a linear equation at the inner level. The process commences with the iterate $(\zeta^n,\omega^n,\psi^n)$ and the order of computation is to first calculate ζ^{n+1}, from which ω^{n+1} is generated, and finally ψ^{n+1} is obtained from ω^{n+1}. The cycle may then be repeated after recomputation of the new velocity field iterate $\underset{\sim}{u}^{n+1}$.

The difference equations (8) for ω^{n+1} and ψ^{n+1} are solved using a secondary inner SOR iteration with empirically estimated optimal relaxation factors of $1.6 \leq \rho_\psi \leq 1.8$ and $\rho_\omega = 1.0$ (as in Davies et al., [11]). Additionally, a necessary consideration for the stability of the outer iteration is to restrict the ω inner iteration to a single iteration per

outer iteration cycle. This is a consequence of the influence of the boundary conditions on ω^{n+1} and applies equally in a Stokesian context (cf. Morton et al. [4]). Utilising graded iterative convergence tolerances with less stringent restrictions on ω than ψ also produces the same effect (see Webster [1]). The essential nature of such practices becomes quite apparent when the residuals of the equations are monitored throughout the iteration process. It is certainly an advantage therefore to be provided with homogeneous boundary conditions on ζ^{n+1}.

The stress ζ^{n+1} is calculated in the following manner. First, the box scheme (9) is introduced for the recirculation zone Ω_h^1. Proceeding in a point-by point fashion starting near B , $\zeta^{n+1}_{i,j+1}$ is given by

$$c_1 \zeta^{n+1}_{i,j+1} + c_2 \zeta^{n+1}_{i,j} + c_3 \zeta^{n+1}_{i+1,j+1} + c_4 \zeta^{n+1}_{i+1,j} = g^n_{i+\frac{1}{2},j+\frac{1}{2}} \qquad (13)$$

where $c_1 = (3\theta-4)\frac{h}{2} - W(u-v)^n_{i+\frac{1}{2},j+\frac{1}{2}}$; $c_m = -\theta\frac{h}{2} \pm W(u \pm v)^n_{i+\frac{1}{2},j+\frac{1}{2}}$, $m = 2, 3, 4$; and $0 \leq \theta \leq 1$. It is vital that Ω_h^1 is restricted to the recirculation zone defined by the known separation line value of ψ^n. Otherwise, large numerical oscillations in ζ^{n+1} occur cross-stream and are subsequently swept upstream. This is due to the sign switch of coefficient c_1 , when v^n begins to dominate u^n. The factor θ may be altered from the average value of unity to the totally weighted zero value dependent upon a pointwise selection criterion; its choice guarantees the stability of the scheme for all variations in $(u-v)^n_{i+\frac{1}{2},j+\frac{1}{2}}$. Second, the Crank-Nicolson scheme (10) is used in Ω_h^2 involving a direct line-by-line marching procedure from outflow to inflow. A tridiagonal matrix of equations results for each I-line and $\underset{\sim}{\zeta}^{n+1}_I$ is related to $\underset{\sim}{\zeta}^{n+1}_{I+1}$ by

$$\left[V\zeta_{j+1} - (U+h(1-\beta))\ \zeta_j - V\zeta_{j-1}\right]_I^{n+1} + \left[V\zeta_{j+1} + (U-\beta h)\,\zeta_j - V\zeta_{j-1}\right]_{I+1}^{n+1}$$

$$= f^n_{I+\frac{1}{2},j} \qquad (14)$$

where $V = \frac{W}{4} v^n_{I+\frac{1}{2},j}$ and $U = W u^n_{I+\frac{1}{2},j}$. A fast tridiagonal solver is used to solve the system of equations (14). Numerical stability of this solver is guaranteed since the associated matrix is diagonally dominant almost everywhere in Ω_h^2, i.e. provided $\left[u^n_{I+\frac{1}{2},j}\right] \geq \frac{1}{2}\left[v^n_{I+\frac{1}{2},j}\right]$ for $\beta = 0$. From a basic 1-D analysis of simple channel flow, the condition $\beta \leq \frac{U}{h}$ must be satisfied to avoid streamwise oscillations in the implementation of the Crank-Nicolson scheme. Furthermore, from a discrete Fourier analysis of the line-by-line marching sweep, the stability criterion $\beta \leq \frac{U}{h} + \frac{1}{2}$ emerges. Both conditions are satisfied and stability affirmed if $\beta = 0$ and $u^n_{I+\frac{1}{2},j} \geq 0$, (see Morton et al., [4]). The Crank-Nicolson scheme is only applicable for a zone predominantly in the x-direction, where streamlines can effectively be tracked. If it is extended to Ω_h^1 a large cross-stream oscillation in ζ^{n+1} is observed due to small velocity field values, and leads to a failure to converge in the Picard iteration.

Relative tolerances in $[\zeta, \omega, \psi]$ of $[10^{-2}, 10^{-2}, 10^{-3}]$ are used to monitor iterative convergence: smoothing of one outer iterate with the next is also used. It is generally observed that, as R is increased, convergence criteria become increasingly more difficult to satisfy. The convergence of the Picard iteration is directly related to R: for small R convergence may be obtained for any W, whilst for larger R (greater than 10) convergence of the Picard iteration deteriorates for larger W. These conclusions are in agreement with the arguments of section 1.

A selection of results is presented in Figs. 3 — 5. For creeping flow ($R = 0$) ζ vanishes $\forall\ W \geq 0$. For $R = 10^{-4}$ solutions are found for $10^{-4} \leq W \leq 10^2$: ζ behaves like $R\underset{\sim}{u}.\underset{\sim}{\nabla}\omega$ for $W \leq \frac{1}{U}$ and like $\frac{R}{W}\omega$ for $W > \frac{1}{U}$, where U is a characteristic velocity value. The same relative behaviour for

ζ is observed for $R \leq 1$. The solutions for ζ for $0.1 \leq W \leq 10$ at $R = 1$ and $R = 10$ are shown for comparison in Fig. 3. For completeness the solutions for ψ and ω are also given at $W = 1$ for $R = 1$ and $R = 10$ in Fig. 4. Solutions for ψ and ω change negligibly with W for $R \leq 1$.

Fig. 5 is included to illustrate the standard tensor stress components p^{ik} (cf. [1]) for the second-order model that arise in the situations investigated. This should dispel any possible confusion arising between these (dependent upon second-order derivatives of $\underset{\sim}{u}$) and the scalar stress ζ (dependent upon third-order derivatives of $\underset{\sim}{u}$). Here the first normal-stress difference $p^{xx} - p^{yy}$ and the shear stress p^{xy} are displayed at $R = 1$ for $W = 1$ and $W = 10$, where normalisation is performed with respect to the corresponding downstream fully-developed wall value.

5. Extension for a Turbulence Model

An initial proposal to utilise the techniques already outlined is to consider the $k \sim \ell$ one equation turbulence energy model as the stress description equation replacing ζ (see Thomas et al. [12]). The model variables are then turbulence energy k, ω and ψ and the model equations are

$$(\underset{\sim}{u}.\underset{\sim}{\nabla} + \gamma k^{\frac{1}{2}})k = \underset{\sim}{\nabla}B.\underset{\sim}{\nabla}k + B\nabla^2 k + \beta k^{\frac{1}{2}} S \ , \quad S = \frac{\partial u_i}{\partial x_j}\left(\frac{\partial u_i}{\partial x_j} + \frac{\partial u_j}{\partial x_i}\right) \ , \tag{15a}$$

$$\underset{\sim}{u}.\underset{\sim}{\nabla}\omega - D\nabla^2\omega = \underset{\sim}{\nabla}.\left(D_x(\psi_{xx}-\psi_{yy}) + 2D_y\psi_{xy} \ , \ 2D_x\psi_{xy} + D_y(\psi_{yy}-\psi_{xx})\right) \ , \tag{15b}$$

$$\nabla^2\psi = -\omega \qquad , \qquad \underset{\sim}{u} = \underset{\sim}{\nabla} \times \psi \ , \tag{15c}$$

where $D = R^{-1} + \beta k^{\frac{1}{2}}$, $B = R^{-1} + \beta\sigma^{-1}k^{\frac{1}{2}}$, $\gamma = c_\mu \beta^{-1}$; $R, \beta, \sigma, \gamma, c_\mu > 0$; and $\beta(\underset{\sim}{x})$ is the length scale given by an assumed algebraic specification. S is noted to be a positive definite field variable.

The treatment of (15a) for k is similar to that for ζ. The positive coefficient γ indicates a switch to marching in the flow direction and there are now additional terms $\underset{\sim}{\nabla}B.\underset{\sim}{\nabla}k$ and $B\nabla^2 k$ to augment the scheme. With reference to Fig. 6a, k_2^{n+1} at point P_2 is calculated by the Crank-Nicolson

scheme as follows: $\partial_x k^{n+1}$ uses $(k_2,k_5)^{n+1}$; $\partial_y k^{n+1}$ uses $(k_1,k_3,k_4,k_6)^{n+1}$; $k^{\frac{1}{2}}k$ is replaced by $(k_5^n)^{\frac{1}{2}}\, k_2^{n+1}$, and $\underset{\sim}{\nabla}B,B$ and $\beta k^{\frac{1}{2}}S$ also use $(k^n)^{\frac{1}{2}}$; $B\,\nabla^2 k$ uses k^{n+1} at $P_1,P_2,P_3,P_4,P_5,P_6,P_8$ and k^n at P_7. A tridiagonal system again emerges with unknowns $(k_1, k_2, k_3)^{n+1}$ at each step. Next with reference to Fig. 6 b, the box scheme is used to calculate k_1^{n+1} within a recirculating flow region. Thus k_1^{n+1} is obtained using $(k_2, k_3, k_4)^{n+1}$ and, additionally, $(k_5, k_6)^n$ for $B\,\nabla^2 k$.

Boundary conditions follow as before except for k and ω at the wall. Here the velocity field near the wall is used to derive such boundary conditions based on the universal logarithmic law of the wall and matching with a viscous sublayer (see Turner, [13]). This necessitates the calculation of the wall shear stress τ_{WALL} from the known velocity field $\underset{\sim}{u}^n$ using the relationships

$$\omega_{WALL} = -R\tau_{WALL} \quad , \quad k_{WALL} = c_\mu^{-\frac{1}{2}} |\tau_{WALL}| \ . \tag{16}$$

Also at attachment and separation points the normal derivative of k at the wall must vanish.

The approach adopted has been to solve laminar flow for $R \leq 2000$, using for the vorticity equation the centred difference scheme of Dennis and Smith [14] with exponential coefficients. Beyond $R = 2000$ the switch to modelling turbulence with the proposed scheme can then be attempted.

The $k \sim \ell$ turbulence model provides an example of a scalar stress equation with the complications arising from a positive coefficient γ. It may therefore be viewed as a forerunner to problems with a stress equation system of similar form, as occurs for Maxwell/Oldroyd fluid models, or indeed for the $k \sim \varepsilon$ turbulence model [15].

6. Conclusions

A finite difference numerical technique has been developed to solve specifically incompressible flow problems of various types. New features involved are the direct marching scheme employed for the stress equation and the particular choice of outer iteration scheme. The study of this and similar iteration schemes has lead to a more complete understanding of their convergence behaviour with respect to the material parameters involved. Indeed, for the second-order model the convergence of the present scheme is directly related to R, and for small R solutions may be obtained for a wide range of W. Extensions of these techniques to further problems with different stress description equations is already in hand and will form the basis of future research.

Acknowledgements

The work reported here forms part of the research programme of the Oxford/Reading Institute for Computational Fluid Dynamics. Particular thanks must go to Professor K. W. Morton, Oxford University and Dr. E. E. Süli, University of Belgrade, for their collaboration in this research.

References

1. Webster, M.F. (1979). Ph.D. thesis (University of Wales).

2. Crochet, M.J. & Pilate, G. Plane Flow of a Fluid of Second Grade through a Contraction. J. Non-Newto nian Fluid Mech. 1, (1976) 247-258.

3. Davies, A.R. Numerical Filtering and the High Weissenberg Number Problem. (1983). J. Non-Newtonian Fluid Mech., to appear.

4. Morton, K.W., Süli, E.E. & Webster, M.F. (1985) In preparation, to appear in Int. J. Num. Meth. Enging.

5. Tanner, R.I. The Stability of so me Numerical Schemes for Model Viscoelastic Fluids. J. Non-Newtonian Fluid Mech. 10, (1982) 169-174.

6. Tanner, R.I. Plane Creeping Flows of Incompressible Second-Order Fluids. Phys. Fluids 9 (I), (1966), 1246-1247.

7. Thom, A. The Flow Past Circular Cylinders at Low Speeds. Proc. Roy. Soc. Lond. A141, (1933), 651-666.

8. Woods, L.C. A Note on the Numerical Solution of Fourth Order Differential Equations. Aeronautical Quarterly 5 (III), (1954) 176.

9. Kawaguti, M. Mathematical Research Centre Report, No. 574, (1965) University of Wisconsin, Madison.

10. Holstein, H. & Paddon, D.J. A Finite Difference Strategy for Re-entrant Corner Flow. In "Numerical Methods for Fluid Dynamics". Academic Press (K.W. Morton & M.J. Baines, Eds.), (1982), pp 341-358, London.

11. Davies, A.R., Walters, K. & Webster, M.F. Long Range Memory Effects in Flows Involving Abrupt Changes in Geometry Part 3: Moving Boundaries. J. Non-Newtonian Fluid Mech. 4, (1979) 325-344.

12. Thomas, C.E., Morgan, K. & Taylor, C. A Finite Element Analysis of Flow over a Backward Facing Step. Comput. Fluids 9, (1981), 265-278.

13. Turner, J.S. "Buoyancy Effects in Fluids". Cambridge University Press, New York and London. (1973).

14. Dennis, S.C.R. & Smith F.T. Steady Flow through a Channal with a Symmetrical Constriction in the Form of a Step. Proc. Roy. Soc. Lond. A372, (1980), 393-414.

15. Launder, B.E. & Spalding, D.B. "Mathematical Models of Turbulence". Academic Press, London and New York. (1972).

Figure Legend

Fig. 1. Schematic flow diagram.

Fig. 2. Mesh near boundary.

Fig. 3. Stress ζ contours.

Fig. 4. Stream function and vorticity contours.

Fig. 5. First normal-stress difference and shear stress.

Fig. 6. Finite difference scheme stencils.

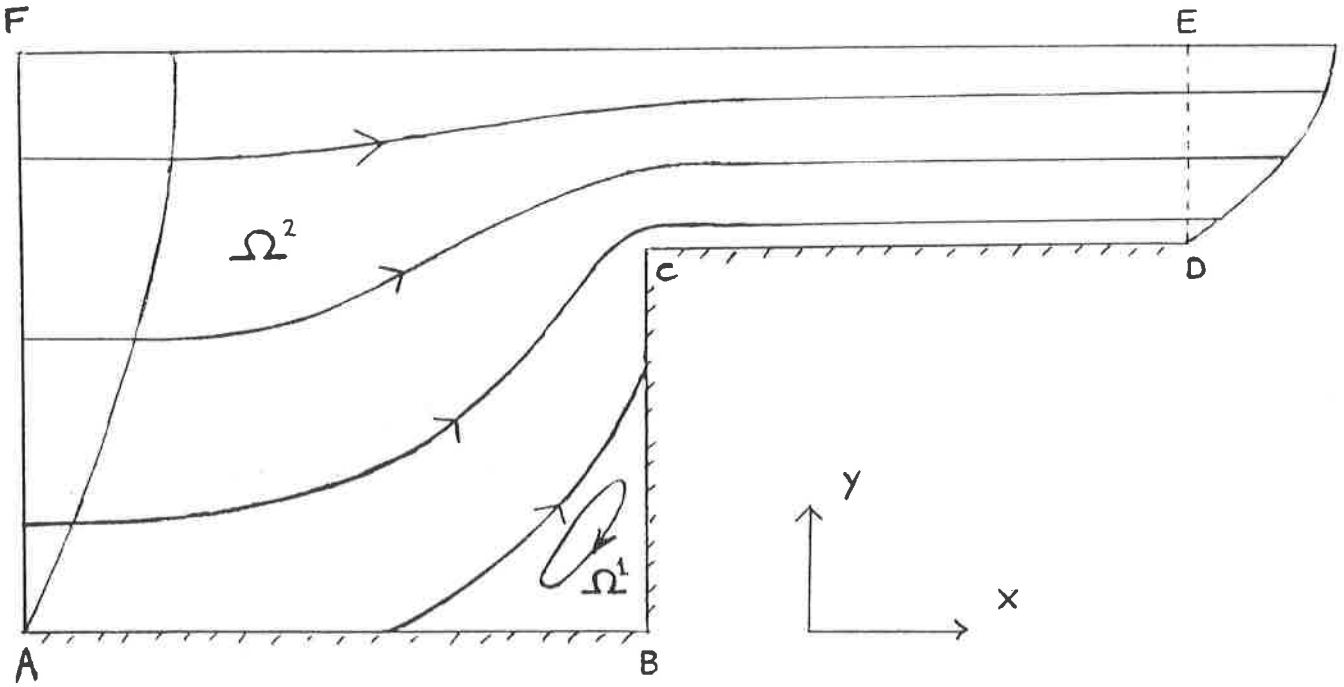

Fig. 1

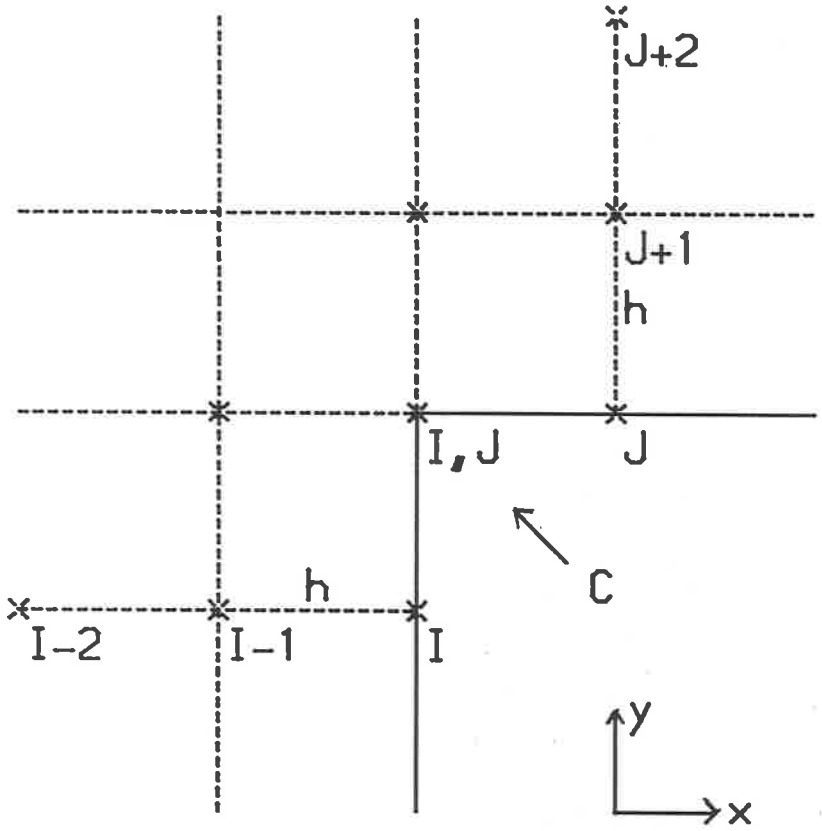

Fig. 2

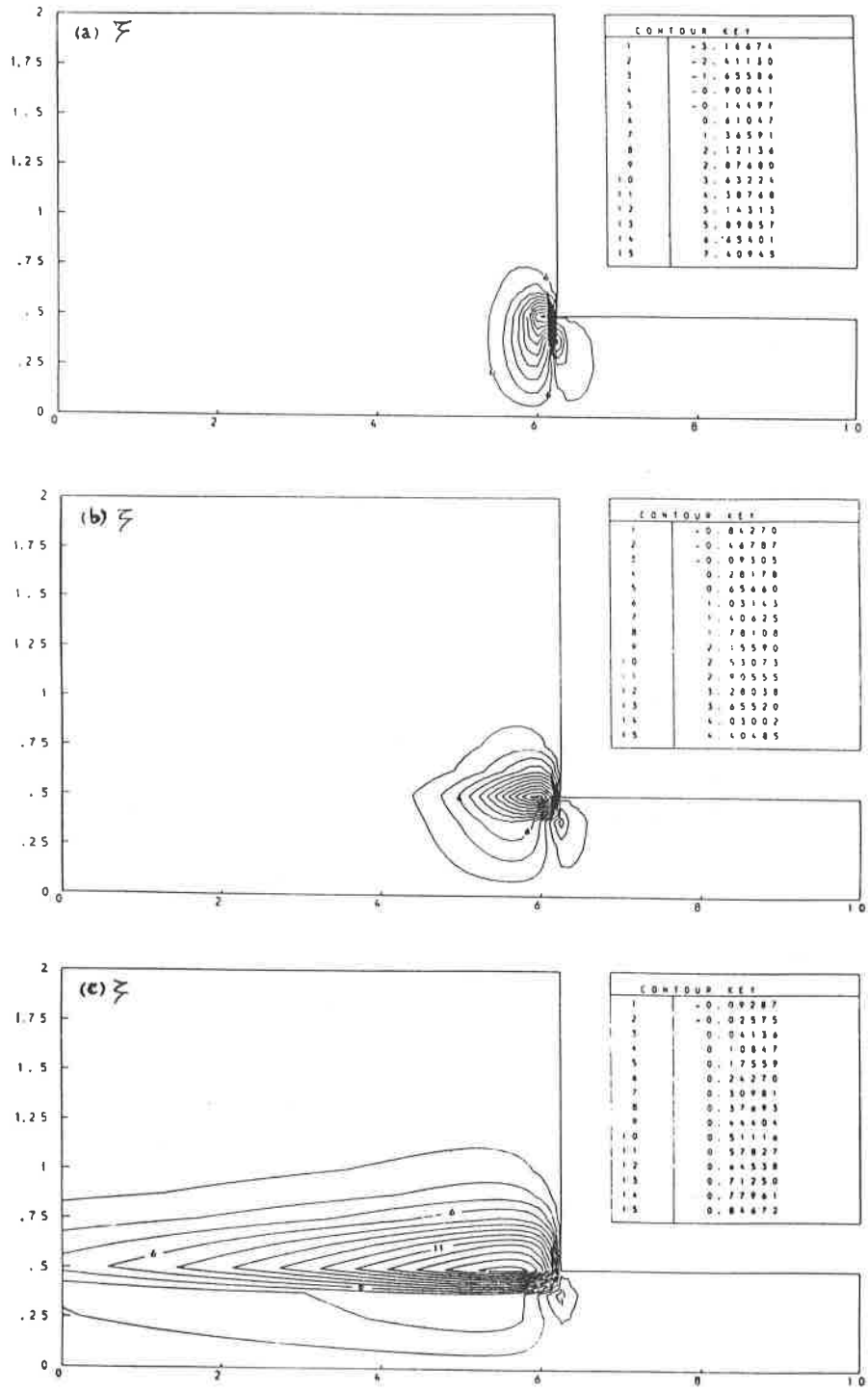

Figure 3. (a)-(c) R = 1 .

(a) W = 0.1 , (b) W = 1 , (c) W = 10 .

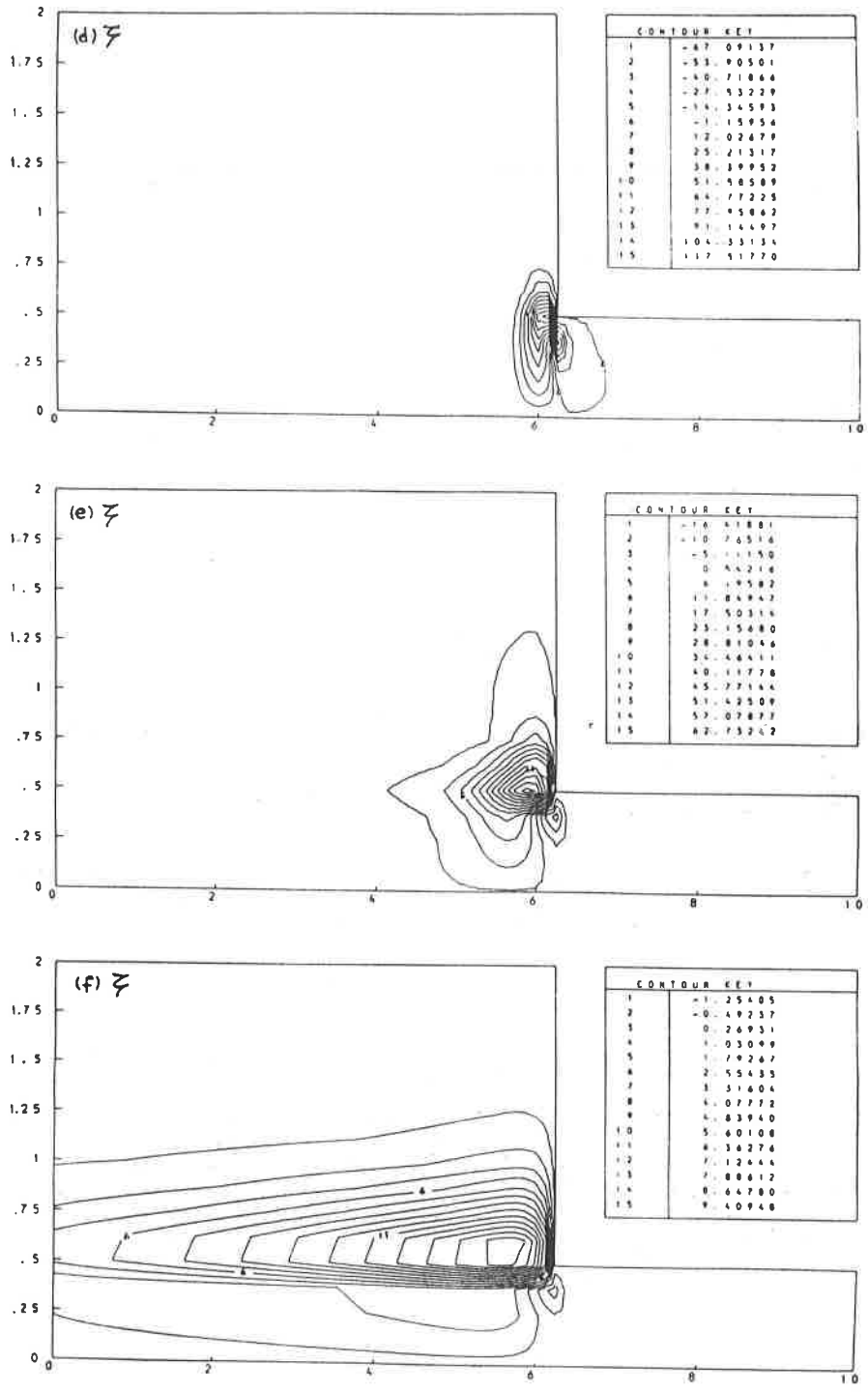

Figure 3. (d)-(f) R = 10 .

(d) W = 0.1 , (b) W = 1 , (c) W = 10 .

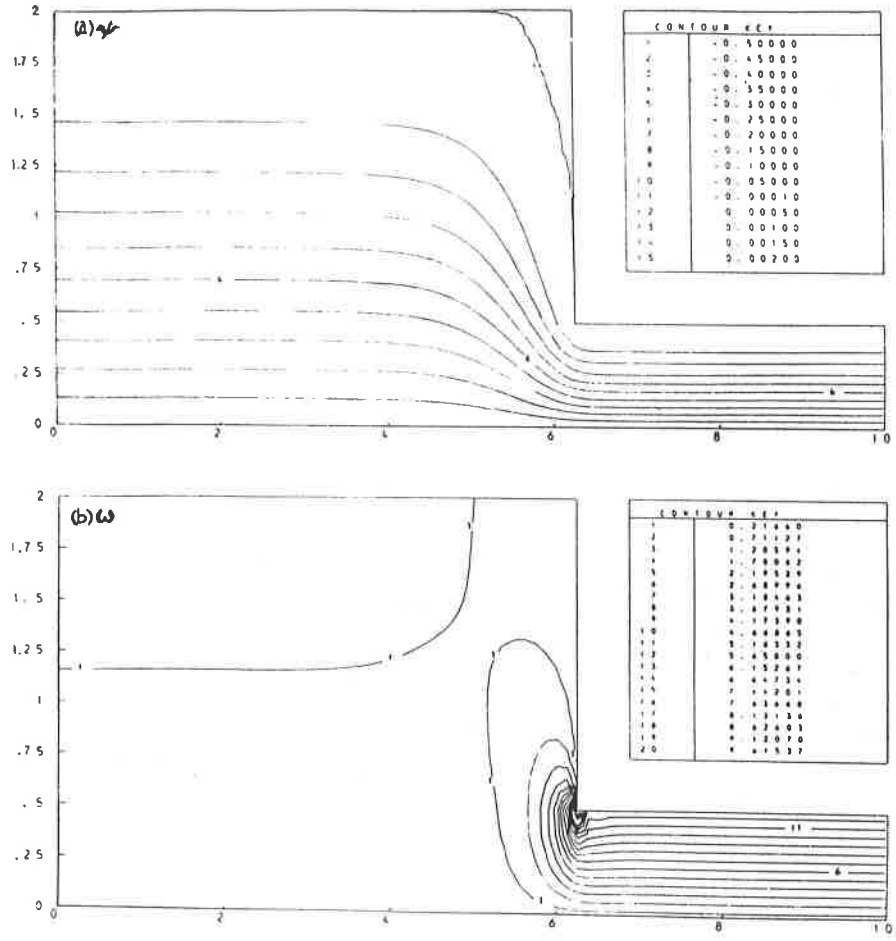

Figure 4. (a), (b) R = 1 , W = 1 .

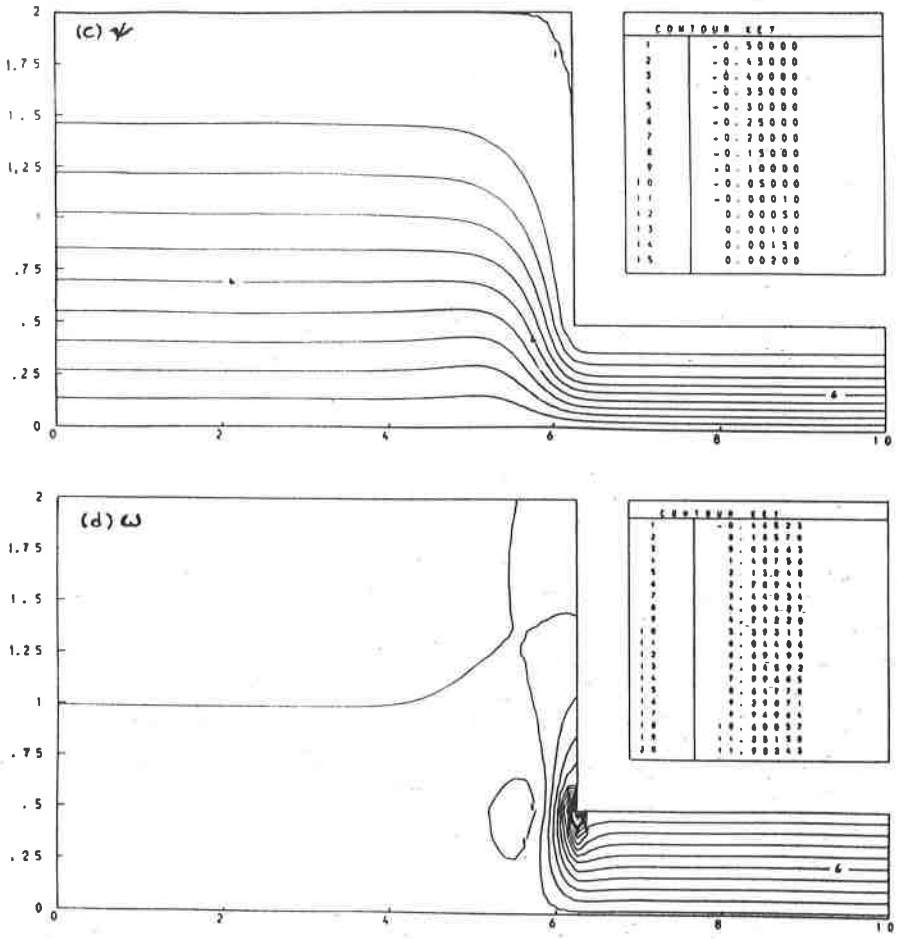

Figure 4. (c), (d) R = 10 , W = 1 .

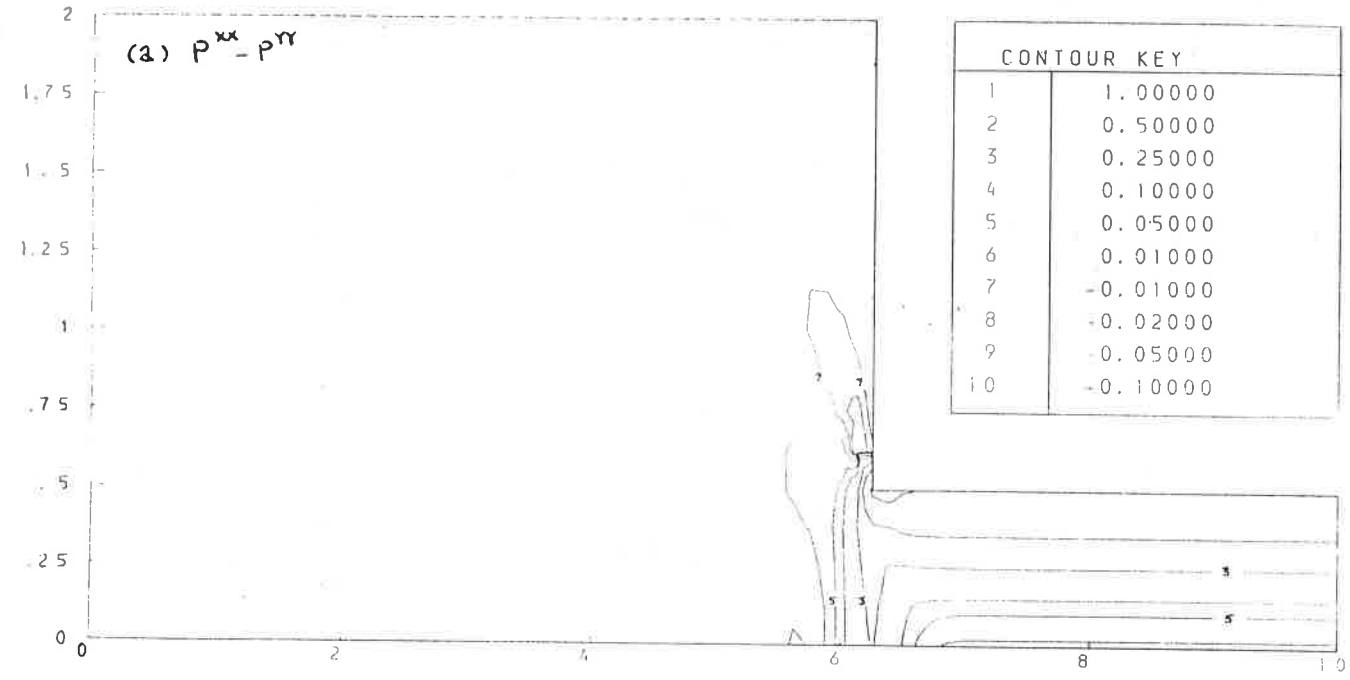

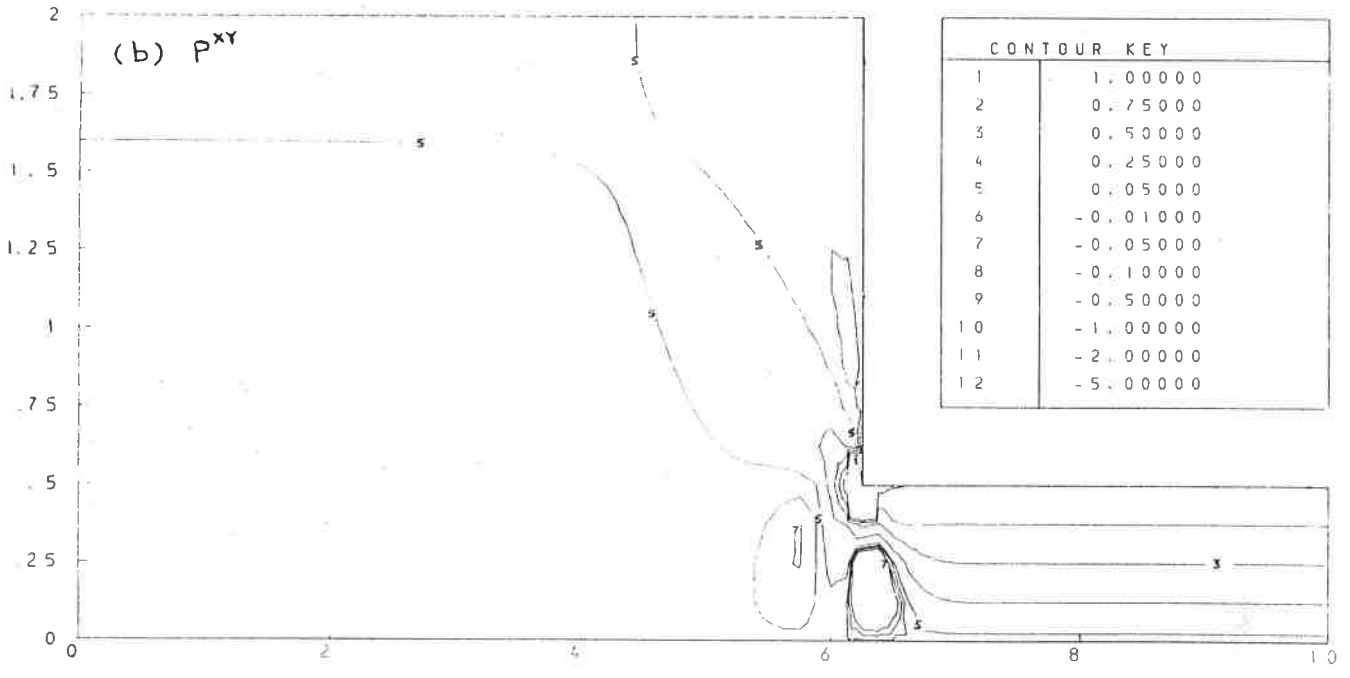

Figure 5. (a), (b) R = 1 , W = 1 .

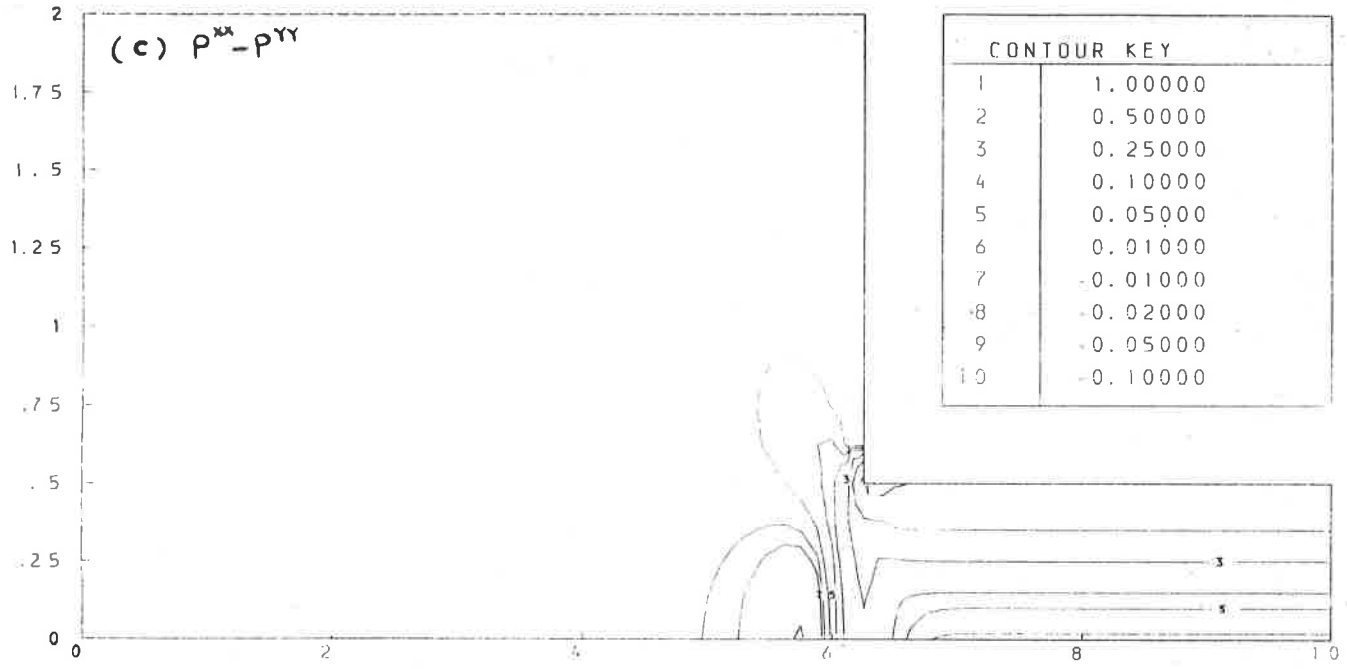

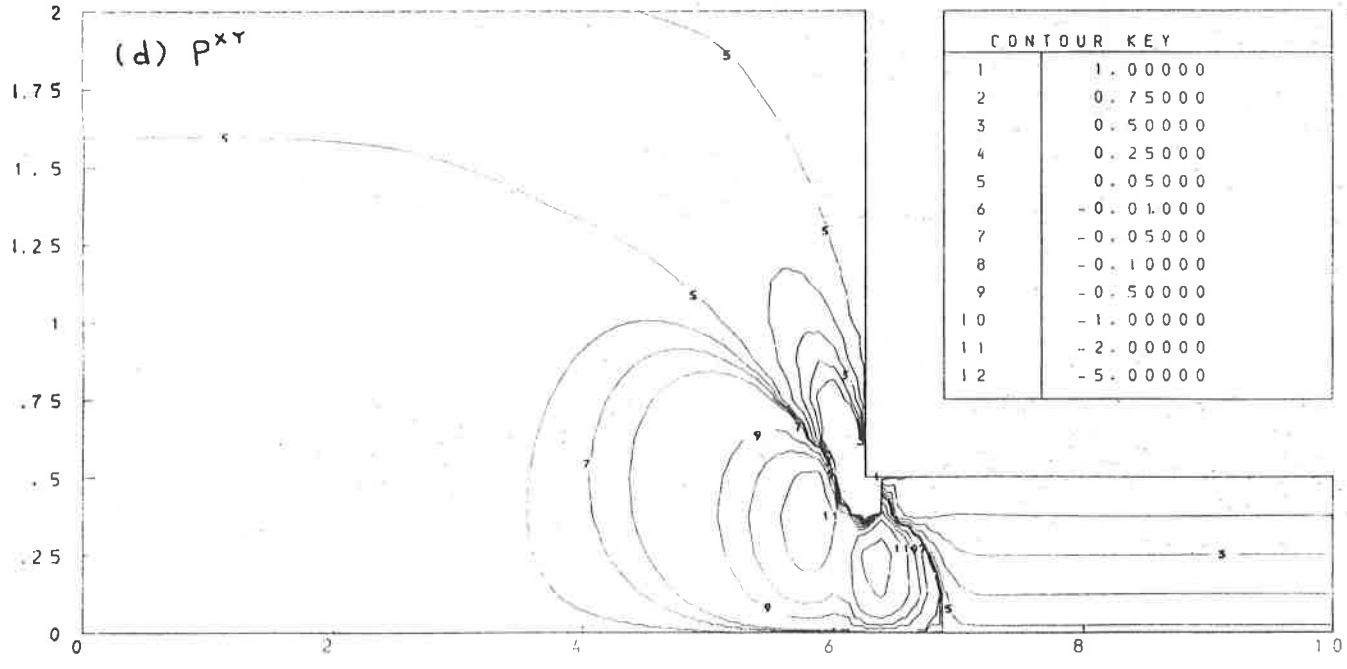

Figure 5. (c), (d) R = 1 , W = 10 .

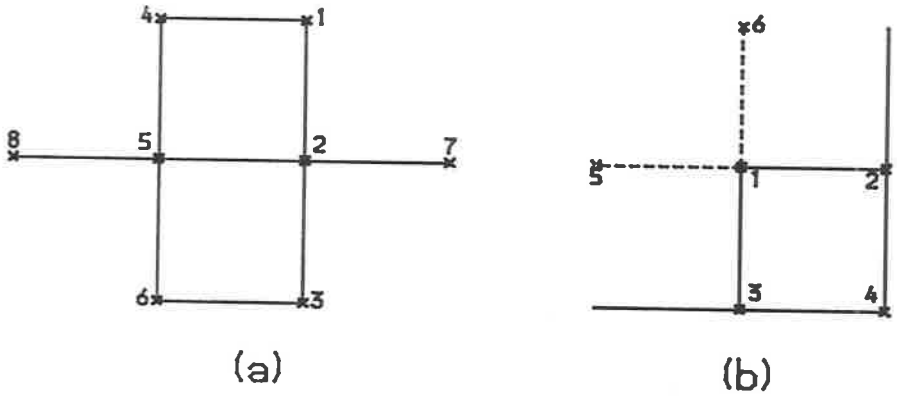

Fig. 6